

Effect of correlated disorder on the magnetism of double exchange systems

G. Bouzerar^{1,2} and O. C epas³

¹Institut N el, d epartement MCBT, 25 avenue des Martyrs, C.N.R.S., B.P. 166 38042 Grenoble Cedex 09, France

²Institut Laue Langevin, BP156, 38042 Grenoble Cedex, France

³Laboratoire de physique th eorique de la mati ere condens ee, C.N.R.S. UMR 7600, Universit e Pierre-et-Marie-Curie, Paris, France

(Received 18 June 2007; published 2 July 2007)

We study the effects of short-range-correlated disorder arising from chemical dopants or local lattice distortions on the ferromagnetism of 3d double exchange systems. For this, we integrate out the carriers and treat the resulting disordered spin Hamiltonian within a local random phase approximation, whose reliability is shown by direct comparison with Monte Carlo simulations. We find large-scale inhomogeneities in the charge, couplings, and spin densities. Compared with the homogeneous case, we obtain larger Curie temperatures (T_C) and very small spin stiffnesses (D). As a result, the large variations of $\frac{D}{T_C}$ measured in manganites may be explained by correlated disorder. We also provide a microscopic model for Griffiths phases in double exchange systems.

DOI: 10.1103/PhysRevB.76.020401

PACS number(s): 75.10.-b, 71.10.-w, 75.47.Lx

Interest in disordered magnetic systems, such as thin magnetic films of transition-metal alloys (Fe-Ni, Co-Ni,...), diluted magnetic semiconductors ($\text{Ga}_{1-x}\text{Mn}_x\text{As}$, $\text{Ge}_{1-x}\text{Mn}_x\text{As}$,...), d^0 materials (HfO_2 , CaO ,...), and or manganites ($R_xA_{1-x}\text{MnO}_3$, where R is a rare-earth ion and A an alkaline ion) has considerably increased during the last decade. One of the reasons is the potential of some of the materials to be incorporated in technological devices. Some of them play a very special role: systems that contain large-scale inhomogeneities. Inhomogeneities can appear during the growth of the sample by molecular beam epitaxy, for example, but can also result from the interplay among many degrees of freedom (charge, spin, orbital, phonons). This is, for example, the case in manganites. It is known that manganites are strongly inhomogeneous at the nanometer scale: (i) large-scale structures in the charge density were seen by electron diffraction of thin films,¹ or tunneling spectroscopy;² (ii) evidence for inhomogeneous spin density was found in neutron diffuse scattering,³ or NMR;⁴ (iii) localized spin waves also suggest the presence of confining potentials.⁵ There is also clear evidence of inhomogeneous structures above T_C , which were interpreted^{6,7} as a Griffiths phase.⁸ Their microscopic origin is one of the central issues of the physics of manganites; it includes phase separation frustrated by long-range Coulomb interactions,⁹ chemical disorders,^{10,11} and polarons.^{12,13}

In this Rapid Communication we argue that the way the disorder is modeled is important to understand large-scale inhomogeneous structures in 3d systems and to explain the Griffiths phase.⁶ For this we consider a model where the disorder is *correlated* at short distances. This model gives a possible explanation for the broad and multimodal distribution of NMR lines,⁴ or the wide distribution of Curie temperatures T_C (Ref. 14) and spin stiffnesses¹⁵ measured in different materials for the same carrier density. The microscopic origin of the correlated disorder could be chemical or polaronic. For instance, in $R_{1-x}A_x\text{MnO}_3$ the dopant A^{2+} which substitutes R^{3+} creates a strong Coulomb potential in its neighborhood and in particular in the eight nearest-neighbor Mn sites surrounding it.¹⁶ This is the model of ‘‘color centers’’ initially discussed by de Gennes.¹⁰ Alterna-

tively, local Jahn-Teller distortions can also be seen as a source of correlated disorder through ‘‘cooperative phonons,’’ which can be mapped onto the same model.

The 3d-correlated disordered double exchange Hamiltonian we consider reads

$$H = \sum_{ij\sigma} (t_{ij}c_{i\sigma}^\dagger c_{j\sigma} + \text{H.c.}) - J_H \sum_i \vec{S}_i \cdot \vec{s}_i + \sum_i \epsilon_i n_i, \quad (1)$$

where $t_{ij} = -t$ for nearest neighbors only, \vec{S}_i is a classical spin localized at site i ($|\vec{S}_i| = 1$), and $\vec{s}_i = c_{i\alpha}^\dagger (\vec{\sigma})_{\alpha\beta} c_{i\beta}$; J_H is the Hund coupling, which is set to ∞ . The on-site potentials ϵ_i may correspond, in particular, to the chemical substitution of R^{3+} by A^{2+} defined by $\epsilon_i = \epsilon_D \sum_l x_l^i$, where the sum runs over the l nearest-neighbor cations of the Mn site i ($l = 1, \dots, 8$) and ϵ_D is the strength of the disorder. We choose randomly x cationic sites for A for which $x_l^i = 1$ (otherwise $x_l^i = 0$). We emphasize that the disorder is correlated because one dopant affects simultaneously the eight nearest-neighbor Mn sites. With these definitions ϵ_i takes the discrete values $0, \epsilon_D, 2\epsilon_D, \dots, 8\epsilon_D$. From stoichiometry, we would expect the hole density n_h to be equal to x , but in order to include the local Jahn-Teller distortion picture as well, we allow them to be different.

The approach we use to study this model is in two steps. First, for a given configuration of disorder we diagonalize Eq. (1) in real space, assuming a fully polarized ground state at zero temperature. This allows us to define an effective Heisenberg Hamiltonian for the classical spins, $H_{\text{eff}} = \sum_{\langle ij \rangle} J_{ij} \vec{S}_i \cdot \vec{S}_j$, where the disordered couplings $\{J_{ij}\}$ are explicitly calculated in the limit $J_H \rightarrow \infty$, using $J_{ij} = t_{ij} \langle c_{i,\uparrow}^\dagger c_{j,\uparrow} \rangle / 2$.^{17,18} In the second step, we diagonalize this Hamiltonian using the self-consistent local random phase approximation (SC-LRPA).¹⁹ It consists of decoupling higher-order spin-spin Green’s functions in the equation of motion. This introduces the local magnetizations $\langle S_i^z \rangle$, which are self-consistently determined by using sum rules. Spatial fluctuations due to disorder are thus treated exactly by solving the equations numerically in real space. This procedure was shown to be reliable to study dilute magnetic semiconductors

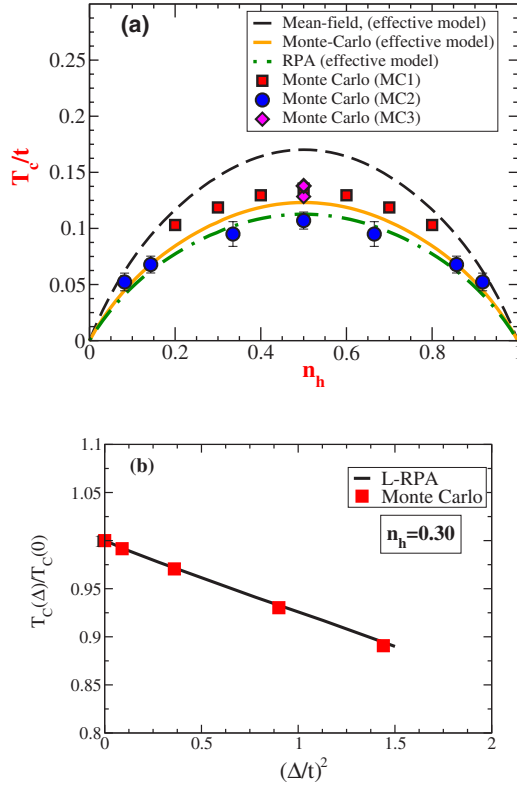


FIG. 1. (Color online) (a) T_C as a function of hole density (clean case). Lines are obtained with the effective Heisenberg Hamiltonian within mean field (dashed line), RPA (dot dashed line), and Monte Carlo (solid line) treatments, and symbols from Monte Carlo simulations of the full double exchange model: MC1 (Ref. 23), MC2 (Ref. 20), and MC3 (Ref. 22) (b) T_C as a function of the on-site potential width Δ for the Anderson disorder (*uncorrelated*): The solid line is obtained with the local RPA and symbols are from Monte Carlo simulations (Ref. 23).

where the couplings were calculated *ab initio*.¹⁹ SC-LRPA provides an analytical expression for T_C and allows us to study much larger systems than those used in Monte Carlo.

In Fig. 1, we test this method by comparing T_C with that of Monte Carlo simulations for both the clean system ($\epsilon_i = 0$) (Refs. 20–23) and the system with Anderson disorder.^{23,24} In the latter case, ϵ_i are *uncorrelated* variables uniformly distributed within $[-\frac{\Delta}{2}, \frac{\Delta}{2}]$. In Fig. 1(a) (clean case), the lines are obtained by studying H_{eff} within a simple mean-field theory, $T_C^{\text{MF}} = 2J$ (dashed line), RPA, $T_C^{\text{RPA}} = 1.32J$ ²⁵ (dot-dashed line), and Monte Carlo simulations, $T_C^{\text{MC}} = 1.44J$ (Ref. 26) (solid line), $J = \frac{-\langle K \rangle}{2z/N}$ where the kinetic energy $\langle K \rangle$ depends on n_h . For the clean system, we recall that $T_C^{\text{RPA}} = 1.32J$ is obtained analytically using $T_C^{\text{RPA}} = \frac{1}{3}(\sum_{\mathbf{q}} \frac{1}{E(\mathbf{q})})^{-1}$, where $E(\mathbf{q}) = zJ[1 - \gamma(\mathbf{q})]$ is the magnon dispersion, z the coordination number, and $\gamma(\mathbf{q}) = \frac{1}{z} \sum_{\mathbf{r}_i} e^{i\mathbf{q} \cdot \mathbf{r}_i}$.²⁵ This expression actually gives a very good approximation of T_C ; the error compared to Monte Carlo calculations is 8%. Now the comparison with Monte Carlo simulations of the full double exchange model (symbols) shows that the difference is within 10%, so the two-step approach is quantitatively reliable. Similarly, when Anderson disorder is added,

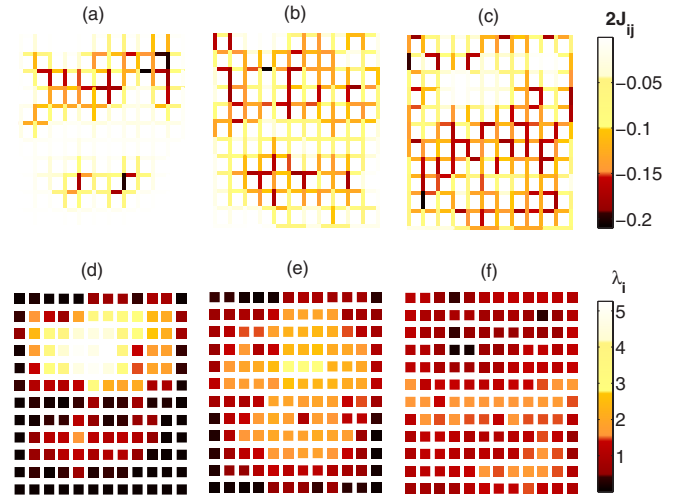


FIG. 2. (Color online) Top row: real-space picture of the magnetic couplings $2J_{ij}$ of the effective model (*correlated* disorder), on one layer of the 12^3 cube. The dark (white) regions correspond to large (weak) couplings. Bottom row: real-space distribution of $\lambda_i = \lim_{T \rightarrow T_C} \frac{\langle S_i^z \rangle}{m}$ on the same layer. From left to right, $n_h = 0.1$ (a),(d), 0.3 (b),(e), and 0.5 (c),(f). Parameters are $x = 0.3$ and $\epsilon_D = 0.15W$.

we have found that the SC-LRPA gives excellent agreement with Monte Carlo data [Fig. 1(b)], stressing that not only are the thermal fluctuations well treated but also the spatial fluctuations due to disorder.

From now on, we consider the model with *correlated* disorder, as discussed above. In Figs. 2(a)–2(c), we have plotted the magnetic couplings J_{ij} in a given layer for various hole densities ($n_h = 0.1, 0.3$, and 0.5 , respectively). They are calculated for a fixed concentration of randomly distributed impurities (color centers), $x = 0.3$, and for a disorder strength, $\epsilon_D = 0.15W$ ($W = 12t$ is the bandwidth), which is chosen to be compatible with *ab initio* calculations.¹⁶ At low density [Fig. 2(a)], the couplings are extremely inhomogeneous in space: we observe large clusters of strong couplings, embedded in regions of weak couplings. The distribution function of $\{2J_{ij}\}$ (not shown) is peaked at $\approx -0.003t$ but has a very long tail up to a cutoff of $-0.3t$ (the average is $\bar{J} = -0.02t$). The regions of strong couplings correspond to hole-rich regions with metallic properties embedded in a hole-poor matrix, which is expected to be insulating, thus leading to phase separation. This tendency will be reinforced if antiferromagnetic superexchange couplings are taken into account; the hole-poor regions will become antiferromagnetic or canted, as observed at very low dopings (droplets in a canted matrix).³ For Anderson disorder, we do not have well-defined nanoscale regions in $3d$,²⁴ unless cooperative phonons were included.²⁷ As the concentration of holes increases, the size of the regions of large couplings increases and the system becomes less inhomogeneous. In this respect, close to half filling ($n_h = 0.5$), the nature of the disorder becomes less important, as we shall see. The reason is that carriers with short Fermi wavelength are less sensitive to the details of the disorder. Spatial inhomogeneities in the magnetization near T_C are directly seen in the distribution of $\lambda_i = \lim_{T \rightarrow T_C} \frac{\langle S_i^z \rangle}{m}$, where m is

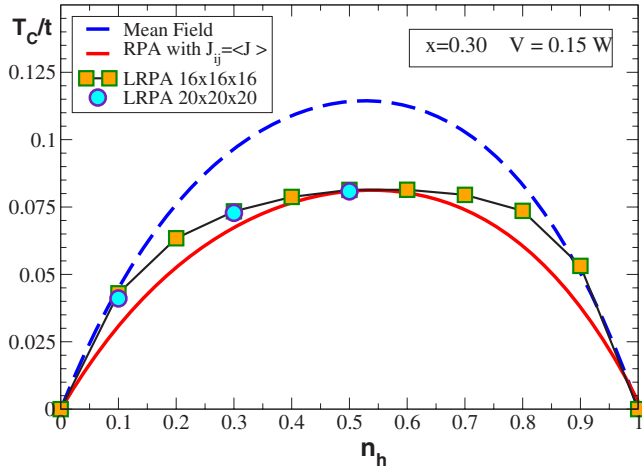


FIG. 3. (Color online) T_C (symbols) as a function of hole density for the model with correlated disorder calculated by SC-LRPA (averaged over 100 configurations of disorder). Also given are the mean-field (dashed line) and RPA with all couplings identical $J_{ij} = \bar{J}$ (solid line). Parameters are $x=0.3$ and $\epsilon_D=0.15W$. Calculations are done for sizes 16^3 and 20^3 .

the averaged magnetization (Fig. 2). For a nearly homogeneous state, λ_i is close to 1, as seen in Fig. 2(f). At low densities, we see a very inhomogeneous texture of λ_i [Fig. 2(d)], with local droplets with λ_i as high as $\approx 4-5$, surrounded by a region with very small local magnetizations. In this case, the distribution of the magnetizations is multimodal. In between [Fig. 2(b)], the droplet increases in size and $\lambda_i \approx 2$ is reduced with respect to Fig. 2(a); the distribution has only one broad peak. These results resemble NMR results where multimodal distributions occur at low dopings and get broader for higher doping.⁴

In Fig. 3, we give T_C averaged over at least 100 disorder configurations (symbols). To see clearly the role of the inhomogeneities, we have also indicated what T_C would be if we replace all couplings by their average, defined by $\bar{J} = \frac{1}{zN} \sum_{ij} J_{ij} = \langle J_{ij} \rangle_{dis}$ (lines). The results are almost identical for n_h close to 0.5 but strongly differ otherwise. Similarly we have found (not shown) that for Anderson disorder, T_C is also extremely close to that of the homogeneous system calculated with \bar{J} . However, at lower hole densities where the couplings are strongly inhomogeneous [Fig. 2(a)], we observe that T_C is larger than that of the homogeneous sample. This happens because of the competition between large (percolating) clusters with couplings much stronger than \bar{J} that tend to increase T_C and thermal fluctuations that reduce it. In particular, at $n_h=0.1$, T_C happens to be close to the mean-field result $T_C^{MF} = 2\bar{J}$ (dashed line), as the result of this competition. It is interesting to remark that this picture is different from the pure percolation picture where thermal fluctuations in the clusters win and reduce T_C ; the difference is that the distribution is much more inhomogeneous here. We note that our T_C is much smaller than that obtained in Ref. 28 where the same model was studied. The reason is that here both spatial and thermal fluctuations are treated beyond the mean-field virtual crystal approximation.

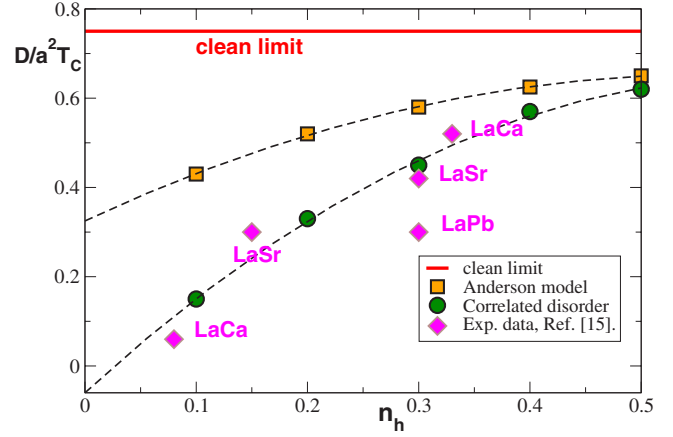


FIG. 4. (Color online) Dimensionless ratio $D/a^2 T_C$ of the spin stiffness to the Curie temperature as a function of the hole density n_h , for the correlated and Anderson forms of disorder. The width of the distribution of potentials was chosen to be the same in both cases: $\epsilon_D=0.15W$ ($x=0.3$) and $\Delta=0.80W$. Experimental results (Ref. 15) are divided by the lattice constant of LaMnO₃ squared ($a=3.9 \text{ \AA}$).

We now argue that this model gives grounds for a Griffiths phase^{6,8} above T_C . As discussed in Ref. 7, correlations in the disorder should enhance the Griffiths phenomenon. Indeed, it is more likely to find large clusters with higher local “Curie” temperatures, as seen in Fig. 2(a). We calculate this temperature T_G from the lowest eigenvalue ϵ of J_{ij} , using $T_G = \frac{1}{3} S(S+1) |\epsilon|$.⁸ Since this is a mean-field estimation, T_G has to be compared to T_C^{MF} . For $n_h=0.1$, we find a large $T_G = 0.11t \approx 2.5T_C^{MF}$. On the other hand, for $n_h \sim 0.5$, the couplings are much more homogeneous, and we have found a much smaller region for the Griffiths phase with $T_G = 0.13t \approx T_C^{MF}$. This is interesting because it shows that T_G is weakly sensitive to n_h . Experimentally this phase seems to occur only in the structurally distorted phase at low dopings,⁷ which suggests that the origin of correlated disorder is the local Jahn-Teller distortions, a case that is also covered by the present model. In fact, it is not clear from our study that we can exclude the chemical origin of the correlated disorder because the Griffiths phase shrinks as we increase the carrier density. A better treatment of thermal fluctuations could possibly lead to the complete disappearance of the Griffiths phase for larger dopings.

We now discuss the effect of the inhomogeneities on the long-wavelength spin excitations at zero temperature. Even in the presence of disorder, these excitations are well defined and characterized by a spin stiffness D ,^{18,29} which is calculated following Ref. 29. Experiments on various manganites show that the dimensionless ratio $D/a^2 T_C$ (a is the lattice constant, taken to be 1 in the following) strongly varies with doping and takes values as small as 0.05 and up to 0.5.¹⁵ This is in contrast with the *clean* double exchange model, where D/T_C is a constant equal to 0.755 [RPA for the simple cubic (sc) lattice²⁵], independent of the hole density. We argue that the measured small values could be explained with a model of correlated disorder, but would require unrealistic large strength of the disorder in the uncorrelated case. Figure 4

gives this ratio, calculated for both models of disorder. Note that to allow for a direct comparison, the width of the distributions of ϵ_i is chosen to be the same. Close to $n_h=0.5$, D/T_C does not really depend on the model, reflecting the absence of the large-scale inhomogeneities we discussed above. When n_h decreases, however, the spin stiffness is dominated by large regions of weak couplings [Fig. 2(a)]: at $n_h=0.10$, D/T_C is 3 times smaller than that obtained with Anderson disorder. In order to get such small values in the Anderson disordered case, one would need a value of Δ much larger than the bandwidth, which would be difficult to reconcile with *ab initio* estimations,¹⁶ on the one hand, and would tend to localize all carriers²⁴ on the other. In Fig. 4 we have also compared our calculations directly with available experimental values.¹⁵ First we note that the overall quantitative agreement does not mean that ϵ_D is quantitatively determined for manganites because other interactions have been neglected here [there is anyway a distribution of ratios for a same doping (see LaSr and LaPb in Fig. 4) for instance, which could be explained by different ϵ_D]. Nevertheless, it is interesting to see that the trend as a function of the hole density is already well captured by taking disorder into ac-

count and that a relatively small amount of *correlated* disorder leads to very small values of D/T_C , contrary to what would be needed in the Anderson case.

To conclude, we have found that short-range-correlated disorder creates large scale spin and charge textures, particularly inhomogeneous at low dopings. Our study suggests that describing the disorder in a more realistic manner may be a key point in understanding experiments, as the occurrence of a Griffiths phase observed for low dopings. In addition, we have found that correlations in the disorder tend to increase T_C because of the presence of large clusters of strong couplings and decrease the spin stiffness D . This results in very small ratios D/T_C , consistent with what has been measured in manganites but hardly compatible with Anderson disorder. The dimensionless ratio D/T_C appears as a good measure of the inhomogeneous character of the magnetic state, a conclusion that may apply beyond manganese oxides.

We thank M. Clusel, M. Hennion, P. Majumdar, Y. Motome, F. Moussa, and S. Petit for stimulating discussions. O.C. thanks the ILL for its hospitality.

-
- ¹M. Uehara, S. Mori, C. H. Chen, and S. W. Cheong, *Nature* (London) **399**, 560 (1999).
- ²M. Fäth, S. Freisem, A. A. Menovsky, Y. Tomioka, J. Aarts, and J. A. Mydosh, *Science* **285**, 1540 (1999).
- ³M. Hennion, F. Moussa, G. Biotteau, J. Rodríguez-Carvajal, L. Pinsard, and A. Revcolevschi, *Phys. Rev. Lett.* **81**, 1957 (1998).
- ⁴G. Allodi, R. De Renzi, and G. Guidi, *Phys. Rev. B* **57**, 1024 (1998); G. Papavassiliou, M. Pissas, G. Diamantopoulos, M. Belesi, M. Fardis, D. Stamopoulos, A. G. Kontos, M. Hennion, J. Dolinsek, J.-Ph. Ansermet, and C. Dimitropoulos, *Phys. Rev. Lett.* **96**, 097201 (2006).
- ⁵M. Hennion, F. Moussa, P. Lehouelleur, F. Wang, A. Ivanov, Y. M. Mukovskii, and D. Shulyatev, *Phys. Rev. Lett.* **94**, 057006 (2005).
- ⁶M. B. Salamon, P. Lin, and S. H. Chun, *Phys. Rev. Lett.* **88**, 197203 (2002); P. Y. Chan, N. Goldenfeld, and M. Salamon, *ibid.* **97**, 137201 (2006).
- ⁷J. Deisenhofer, D. Braak, H.-A. Krug von Nidda, J. Hemberger, R. M. Eremina, V. A. Ivanshin, A. M. Balbashov, G. Jug, A. Loidl, T. Kimura, and Y. Tokura, *Phys. Rev. Lett.* **95**, 257202 (2005).
- ⁸A. J. Bray, *Phys. Rev. Lett.* **59**, 586 (1987).
- ⁹A. Moreo, S. Yunoki, and E. Dagotto, *Science* **283**, 2034 (1999); E. Dagotto, *Nanoscale Phase Separation and Colossal Magnetoresistance* (Springer, Berlin, 2002).
- ¹⁰P.-G. de Gennes, *Phys. Rev.* **118**, 141 (1960).
- ¹¹E. L. Nagaev, *Phys. Rep.* **346**, 387 (2001).
- ¹²T. V. Ramakrishnan, H. R. Krishnamurthy, S. R. Hassan, and G. Venketeswara Pai, *Phys. Rev. Lett.* **92**, 157203 (2004).
- ¹³V. B. Shenoy, T. Gupta, H. R. Krishnamurthy, and T. V. Ramakrishnan, *Phys. Rev. Lett.* **98**, 097201 (2007).
- ¹⁴H. Y. Hwang, S.-W. Cheong, P. G. Radaelli, M. Marezio, and B. Batlogg, *Phys. Rev. Lett.* **75**, 914 (1995).
- ¹⁵J. A. Fernandez-Baca, P. Dai, H. Y. Hwang, C. Kloc, and S.-W. Cheong, *Phys. Rev. Lett.* **80**, 4012 (1998), and references therein; see also T. Chatterji, L. P. Regnault, P. Thalmeier, R. van de Kamp, W. Schmidt, A. Hiess, P. Vorderwisch, R. Suryanarayanan, G. Dhalenne, and A. Revcolevschi, *J. Alloys Compd.* **326**, 15 (2001).
- ¹⁶W. E. Pickett and D. J. Singh, *Phys. Rev. B* **55**, R8642 (1997).
- ¹⁷K. Kubo and N. Ohata, *J. Phys. Soc. Jpn.* **33**, 21 (1972).
- ¹⁸Y. Motome and N. Furukawa, *Phys. Rev. B* **71**, 014446 (2005).
- ¹⁹G. Bouzerar, T. Ziman, and J. Kudrnovsky, *Europhys. Lett.* **69**, 812 (2005).
- ²⁰S. Yunoki, J. Hu, A. L. Malvezzi, A. Moreo, N. Furukawa, and E. Dagotto, *Phys. Rev. Lett.* **80**, 845 (1998).
- ²¹M. J. Calderon and L. Brey, *Phys. Rev. B* **58**, 3286 (1998).
- ²²J. L. Alonso, L. A. Fernández, F. Guinea, V. Laliena, and V. Martín-Mayor, *Nucl. Phys. B* **596**, 587 (2001).
- ²³Y. Motome and N. Furukawa, *Phys. Rev. B* **68**, 144432 (2003).
- ²⁴S. Kumar and P. Majumdar, *Phys. Rev. Lett.* **91**, 246602 (2003).
- ²⁵H. B. Callen, *Phys. Rev.* **130**, 890 (1963).
- ²⁶K. Chen, A. M. Ferrenberg, and D. P. Landau, *Phys. Rev. B* **48**, 3249 (1993).
- ²⁷S. Kumar, A. P. Kampf, and P. Majumdar, *Phys. Rev. Lett.* **97**, 176403 (2006).
- ²⁸J. Salafranca and L. Brey, *Phys. Rev. B* **73**, 214404 (2006).
- ²⁹G. Bouzerar, arXiv:cond-mat/0610465 (unpublished).